PCCP

ROYAL SOCIETY OF CHEMISTRY

PAPER

Cite this: DOI: 10.1039/d3cp00542a

Fluorescence profiles of water droplets in stable levitating droplet clusters†

Alexander A. Fedorets, [a] Eduard E. Kolmakov, [a] Dmitry N. Medvedev,[a] Michael Nosonovsky *[ab] and Leonid A. Dombrovsky [ac]

Received 3rd February 2023,
Accepted 13th May 2023

DOI: 10.1039/d3cp00542a

rsc.li/pccp

Clusters of nearly identical water microdroplets levitating over a locally heated water layer are considered. The high-resolution and high-speed fluorescence microscopy showed that there is a universal brightness profile of single droplets, and this profile does not depend on the droplet temperature and size. We explain this universal profile using the theory of light scattering and propose a new method for determining the parameters of possible optical inhomogeneity of a droplet from its fluorescent image. In particular, we report for the first time and explain the anomalous fluorescence of some large droplets with initially high brightness at the periphery of the droplet. The disappearance of this effect after a few seconds is related to the diffusion of the fluorescent substance in water. Understanding the fluorescence profiles paves the way for the application of droplet clusters to the laboratory study of biochemical processes in individual microdroplets.

1. Introduction

Self-assembled clusters of condensed monodisperse water microdroplets levitating in an ascending flow of humid air over a locally heated water surface are a relatively recently discovered phenomenon.[1–5] Droplet clusters are similar to such classical objects of colloid chemistry as colloid crystals and dust crystals; however, they possess many unique features absent from the latter. It is known that organic chemical reactions are accelerated when reactants are present in microdroplets. The reaction rate may increase by orders of magnitude with decreasing droplet size. This phenomenon has long attracted the attention of researchers but remains insufficiently studied.[6–8] Clusters can be used for the laboratory study of biochemical processes in individual droplets with optical diagnostics methods.

Detailed laboratory observations and measurements of chemical reactions in levitating microdroplets with dissolved substances require stabilization of droplets' position in space, size, and temperature. The traditional procedure of cluster generation implies spontaneous condensation of droplets from water vapor. An alternative method is when independently generated small droplets are delivered to an area above a heated water layer, where the droplets form a levitating cluster and grow due to the condensation of the vapor from an upward flow of humid air. The latter method has already been used by Fedorets *et al.*[9] to study the first observed self-stabilization of a cluster of pure water droplets levitating over a layer of water containing a small amount of salt. The obvious advantage of such a more flexible procedure compared to the spontaneous formation of a droplet cluster over the heated water surface is that it is possible to generate clusters with droplets of different chemical compositions.

The transition to biochemical experiments in microdroplets requires special methods of optical diagnostics ranging from relatively simple to hyperspectral imaging.[10–12] Fluorescence microscopy is used in the initial stage of work. The method described in[13–15] has been used in diverse studies, mainly in chemistry, biology, and medicine resulting in recent publications on the study of processes in small droplets and their groups that have caused the greatest interest of the authors.[16–21] Fluorescence microscopy is used for a wide range of biochemical and biomedical studies, including, for example, the analysis of the blood–brain barrier for the rational design of new drugs.[22,23]

In the present paper, we will present the flexible experimental procedure for the generation of stable clusters levitating microdroplets of water with dissolved substances or suspended microorganisms and will study the possibilities of modern fluorescent microscopy as a method of diagnostics of processes occurring in semitransparent microdroplets. We will present new results on the fluorescence of microdroplets of water,

[a] X-BIO Institute, University of Tyumen, 6 Volodarskogo St, Tyumen, 625003, Russia. E-mail: fedorets_alex@mail.ru, e.e.kolmakov@utmn.ru, dn.medv@yandex.ru
[b] University of Wisconsin-Milwaukee, 3200 N Cramer St., Milwaukee, WI 53211, USA. E-mail: nosonovs@uwm.edu
[c] Joint Institute for High Temperatures, 17A Krasnokazarmennaya St., Moscow, 111116, Russia. E-mail: ldombr@yandex.ru

† Electronic supplementary information (ESI) available. See DOI: https://doi.org/10.1039/d3cp00542a

which enable us to determine a universal fluorescence profile of a homogeneous droplet that is independent of the droplet size and its temperature. An interesting physical effect was discovered, which was shown to be related to the low diffusion rate of the fluorescent substance in water. In large water droplets formed by the merger of two droplets, an anomalous brightness profile of fluorescence with a maximum at the periphery of the droplet was observed for the first time. As one might expect, the diffusion of fluorescein led to a fairly rapid blurring of the anomalous profile and the formation of the universal fluorescence profile.

2. Experimental procedure

The experiments were performed on a laboratory setup described recently by Fedorets *et al.*[9,24] A thin layer of water in the central part of the cuvette was heated from a substrate illuminated from below by a laser beam with adjustable power of radiation. The working volume of the setup with the main elements, including external infrared radiation to stabilize the droplet sizes[25,26] is shown schematically in Fig. 1a. The cluster was printed from an aqueous solution of sodium fluorescein (uranine) with a concentration of 3 mg l^{-1} by injecting microdroplets with a piezoelectric dispenser (MicroFab, USA), see Fig. 1b.

A Hyper E600 LED illuminator (YODN, Taiwan) and an Axio Zoom.V16 stereo microscope (Zeiss, Germany) with a four-position turret for optical cubes were used in the experiments. Zeiss Fs09 and Chroma 39010 filter sets were used, whose optical parameters allow recording fluorescein luminescence with the maximum absorption and fluorescence at wavelengths λ = 0.490 μm and 0.515 μm.[27] Video recording at 15 fps was performed with an iXon Ultra 888 fluorescence microscopy camera (Andor, UK). Four miniature EK-8520 infrared thermal sources (Helioworks, USA) were used to stabilize the cluster. Parameters of EK-8520 radiation can be found in ref. 25. The radiation sources were placed symmetrically relative to the vertical axis of the cluster, at an angle of 23° to the horizontal plane, and were oriented so that the axis of the radiation beam passed through the droplet cluster. As a result, the droplets and the water layer under the cluster were illuminated almost uniformly. The temperature of the water surface under the cluster, T_{surf}, was monitored with a CTL-CF1-C3 pyrometric sensor (Micro-Epsilon, USA).

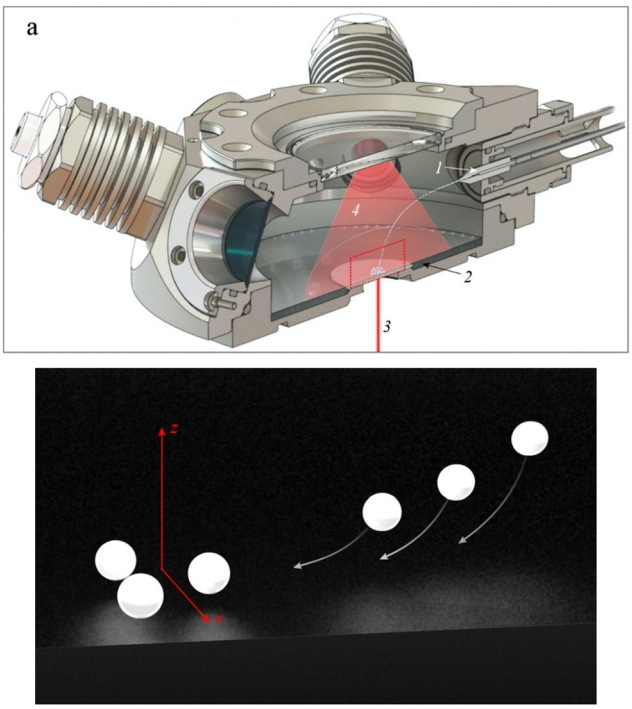

Fig. 1 (a) Schematic representation of the working volume: 1 – piezoelectric dispenser, 2 – water layer in a metal cuvette, 3 – laser beam, 4 – infrared radiation; (b) injected droplets (right) form a droplet cluster (left).

The experiments were carried out at a constant total radiative flux from infrared sources q_{IR} = 11.2 kW m^{-2}. Five levels of laser power were selected, at which T_{surf} = 65 °C, 70 °C, 75 °C, 80 °C, and 85 °C (with an accuracy of ±1 °C). In all experiments, the temperature at the periphery of the water layer was maintained at 10 °C by cooling the cuvette with a Piccolo 280 OLÉ cryothermostat (Huber, Germany). It is important to note that even at T_{surf} = 65 °C, the humid air flow velocity was sufficient to prevent spontaneously condensing droplets from penetrating into the cluster. Because of this, the cluster consists only of initially injected droplets during the experiment.

The developed computer program makes it possible to determine the parameters of all cluster droplets from video frames during the experiment: to measure their radius a and volume v, as well as to obtain the distribution of fluorescence brightness over the droplet cross-section. As the main characteristic of droplet fluorescence, the average brightness of the image of the droplet center I (the central pixel and eight pixels adjacent to it) is used. Unless specifically noted, I, a, and v are obtained by averaging over all droplets in the cluster. In the original images, the brightness is measured in conventional units encoded by the camera.

3. Experimental results

The images in Fig. 2 show the evolution of the cluster of fluorescent droplets at T_{surf} = 70 °C (see also Video S1, ESI†). Hereinafter, the time reference point t_0 is considered to be the moment of complete cluster assembly, from which the cluster contains 16 droplets until the end of the recording, although 0.7 s before t_0 the cluster is still forming (the flying droplets are visible in the upper left corner of the image). The noticeable decrease in the brightness of the droplet fluorescence at $t = t_0 + 5$ s will be discussed below.

The equilibrium droplet size obtained by infrared irradiation may differ from the size of the injected droplets. Therefore, when analyzing the measurement results, the change in the dissolved substance's initial concentration must be considered. Fig. 3 shows experimental values of the normalized droplet volume change rate $\bar{u}_v = u_v/v_o$ (v_o is the initial volume of the droplet) from water layer surface temperature during the first

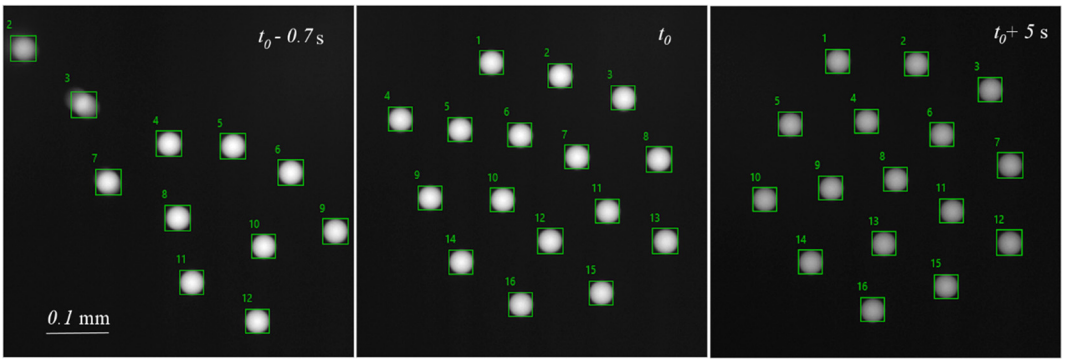

Fig. 2 Formation of a cluster from droplets injected by the dispenser.

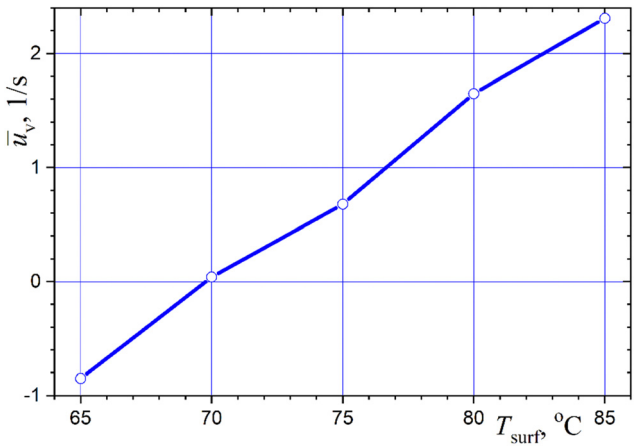

Fig. 3 Effect of water layer surface temperature on the droplet volume change rate.

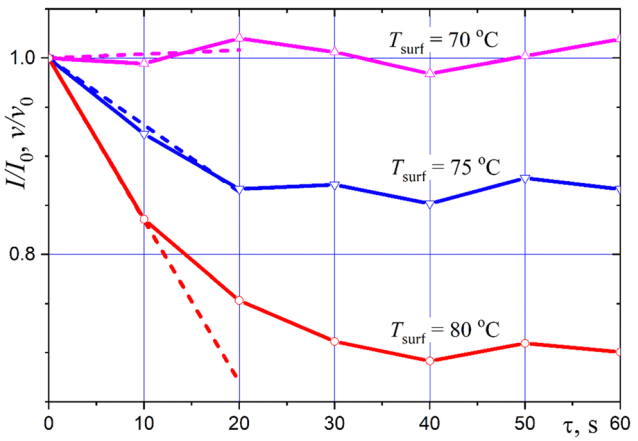

Fig. 4 Effect of the illumination pause τ on the fluorescence intensity of the droplet cluster. The dashed straight lines are the dependences of v/v_0 on τ.

ten seconds of observation when droplet size changes most rapidly. A negative value of $\bar{u}_v$ at T_{surf} = 65 °C indicates a decrease in the initial droplet size when reaching the equilibrium value. It turned out that at T_{surf} = 70 °C under experimental conditions the initial and equilibrium droplet sizes are almost the same, which is very useful for experiments sensitive to changes in the initial concentration of the dissolved substance.

To understand the temperature dependency, experiments were performed at different values of T_{surf} with the droplet illumination turned off immediately after completion of cluster formation for time τ, varying from 10 to 60 s. The results obtained are shown in Fig. 4. One can see that at T_{surf} = 70 °C fluorescence of droplets after a pause in illumination is almost independent of the pause duration (the scatter is within the experimental error). At higher temperatures of the water surface increasing τ at first leads to a decrease of I/I_0, proportional to the rate of condensational growth of droplets, and then the fluorescence intensity comes to a constant value. This result means that the weakening of fluorescence is not due to the thermal decomposition of fluorescein, but is due only to a decrease in its concentration during the growth of droplets.

Fig. 5 shows the dependence of the logarithm of the relative fluorescence intensity of cluster droplets on time at T_{surf} = 85 °C, when the effect of condensational growth of droplets is maximum. The initial part of the curve is well approximated by a linear function, which means that the

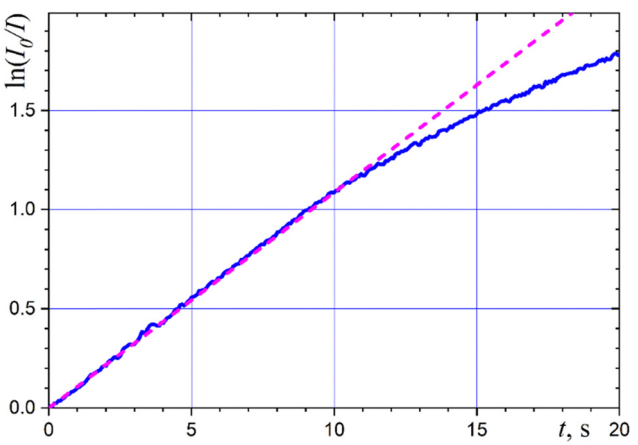

Fig. 5 Variation of water droplet fluorescence intensity over time at T_{surf} = 85 °C: solid line – measurement results, dashed line – linear approximation by the first ten seconds.

fluorescence decreases exponentially with time. The deviation of the curve from the initial linear dependence can be explained by the multistep reaction mechanism,[28–30] but the study of the kinetics of fluorescein fading is beyond the scope of this study. Note that, according to Imamura and Koizumi,[31] the use of the conventional first-order reaction works only in the case of a much more dilute solution than the one used in our experiments.

Similar experiments at different values of water layer surface temperature showed very close fluorescein fading rates in droplets. The found values of the fading rate differed from the average value by ±4% in the range $65 < T_{surf} < 85$ °C, which can be attributed to measurement error. This result supports the conclusion that there is no thermal decomposition of fluorescein in the cluster droplets.

Fig. 6 shows the dependences of the normalized rate of fluorescein fading $\bar{u}_f$ on the dimensionless power $\bar{P} = P/P_{max}$ of the light source that excites the fluorescence of cluster droplets and a 400 μm thick water layer. The measurements were made at $T_{surf} = 70$ °C and the same concentration of fluorescein in the droplets and in the water layer. Despite the discrepancy between the measurements using different optical cubes, the main result is evident and does not depend on the light source power: the fading rate of fluorescein in microdroplets is 3–3.5 times higher than in a relatively thick water layer. The obtained result means that photochemical reactions in the illuminated microdroplets proceed much faster than in a relatively thick layer of water, which agrees with the general conclusion by Li *et al.*[8]

In most experiments, the brightness profile did not undergo qualitative changes from the moment the droplet was embedded in the cluster and throughout the observation time. However, droplets with anomalous nonmonotonic brightness profiles were also observed. Such droplets can be seen in Fig. 7, which shows images of the same cluster of droplets at T_{surf} = 70 °C at different moments of time.

To compare the fluorescence profiles of droplets of different radii is a and with different fluorescence intensities, two variants of normalization are convenient:

$$\bar{I}_1(\bar{r}, t) = \frac{I(\bar{r}, t)}{I_{00}} \quad I_{00} = I(0, 0), \tag{1}$$

$$\bar{I}_2(\bar{r}, t) = \frac{I(\bar{r}, t) - I_b}{I_0 - I_b}, \quad I_0 = I(0, t) \tag{2}$$

where $\bar{r} = r/a$ is the dimensionless radial coordinate and I_b is the background brightness. The normalized brightness profiles of fluorescence are important source of information about the processes in the droplet. Fig. 8 shows both monotonic ("normal", Fig. 8a for droplet 16) and initially nonmonotonic ("abnormal", Fig. 8b for droplet 48) brightness profiles $\bar{I}_1(\bar{r},t)$ at water layer surface temperature T_{surf} = 70 °C. One can see in Fig. 8b that after about 6 s the initially nonmonotonic brightness profile becomes monotonic. Interestingly, the maximum brightness in the nonmonotonic profile increases as it moves toward the central part of the droplet. This looks like the propagation of a zone of increased fluorescein concentration as the volume of this spherically symmetric zone decreases with the decrease in radius.

It is obvious that monotonic profiles are similar to each other and normalization (2) leads to their almost complete coincidence (see Fig. 9 for droplet 16). The latter means that we can speak of a universal brightness profile $\bar{I}_2(\bar{r},t)$, which is independent of the droplet radius and fluorescence brightness. It is natural to assume that the universal profile corresponds to a uniform fluorescein concentration in the droplet.

Fluorescence intensity is known to depend on liquid temperature, which finds application in microfluidics.[32] At first glance, the temperature profile in the droplet may lead to an abnormal fluorescence profile if one assumes that the initially cooler droplet is heated from the surface while being join the cluster. However, simple estimates show that the time of temperature smoothing in the droplet due to the heat conduction of water is orders of magnitude shorter than the time of evolution of the anomalous fluorescence profile. Thus, the thermal nature of the anomalous fluorescence is ruled out. Apparently, in anomalously fluorescing large droplets we are dealing with a much slower diffusive smoothing of the fluorescein concentration after the merging of two droplets, one of which is a droplet of pure water formed by steam condensation over the surface of the heated water layer. Indeed, according to Casalini *et al.*,[33] the diffusion coefficient of fluorescein in water is $D = 0.42 \times 10^{-9}$ m^2 s^{-1}, and the time of smoothing of the fluorescein concentration in a droplet of radius $a \approx 32$ μm is $\tau_D = a^2/D \approx 2.5$ s, which agrees well with the experimental data (see Fig. 8).

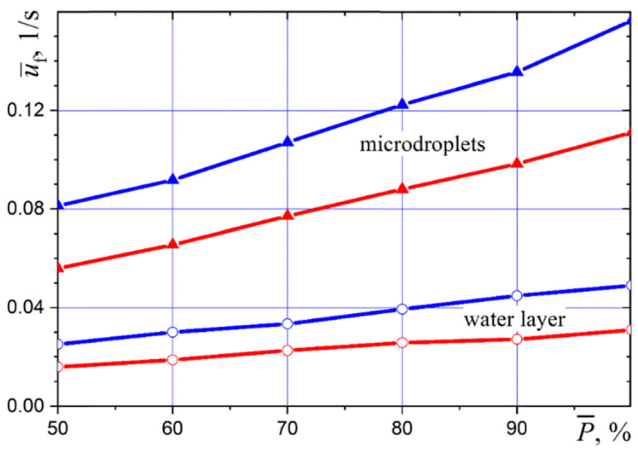

Fig. 6 The difference between the fluorescence of cluster microdroplets and water layer. Measurements using the optical cubes Chroma 39010 (red curves) and Zeiss Fs09 (blue curves).

4. Universal fluorescence profile

The observed universal profile of fluorescence of a water droplet at a uniform distribution of fluorescein over the droplet volume is formed as a result of two optical effects. First, when a spherical droplet is illuminated from one side with a parallel beam of light of uniform intensity, its absorption in the droplet is far from uniform. Second, the droplet's fluorescence profile,

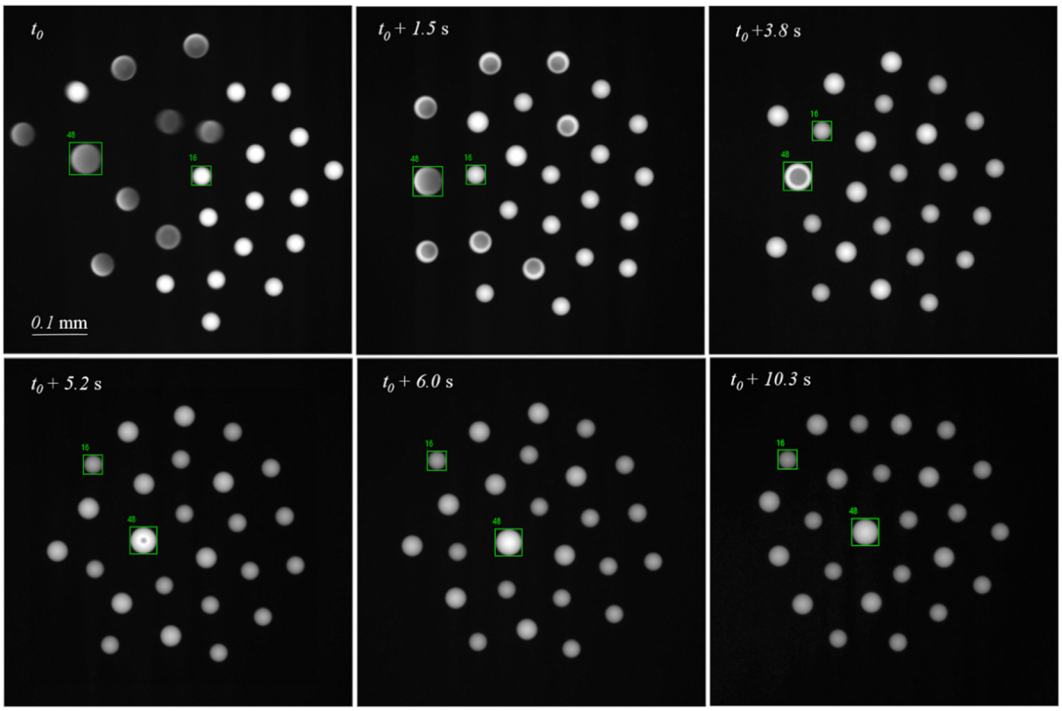

Fig. 7 A cluster of droplets with normal and abnormal fluorescence.

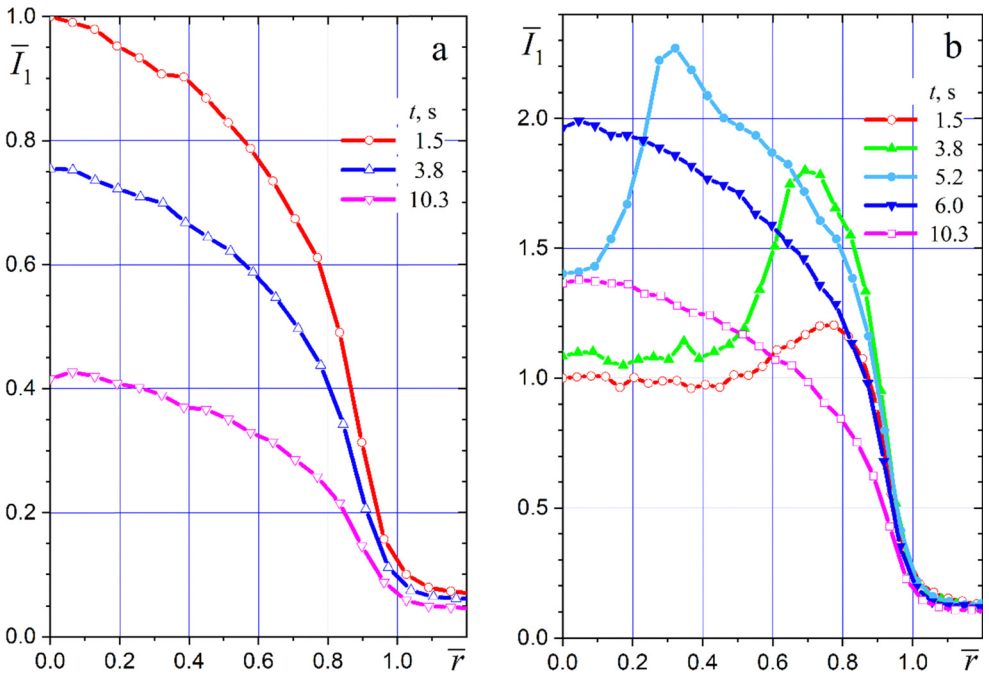

Fig. 8 Changes in the droplet fluorescence profile over time: (a) normal droplet 16, (b) abnormal droplet 48.

which is proportional to the power of the absorbed light, is formed as a result of the refraction and reflection of the emitted light on the surface of the droplet.

The light absorption in a homogeneous semitransparent spherical particle or droplet of arbitrary size can be calculated using a rigorous Mie solution.[34–36] As the particle size increases (this size is characterized by the diffraction parameter $x = 2\pi a/\lambda$, where a is the particle radius and λ is the wavelength of the incident light), the general solution degenerates and does not depend on the diffraction parameter. This asymptotic solution is described by the geometrical optics approximation. Strictly speaking, the wave effects do not disappear completely but

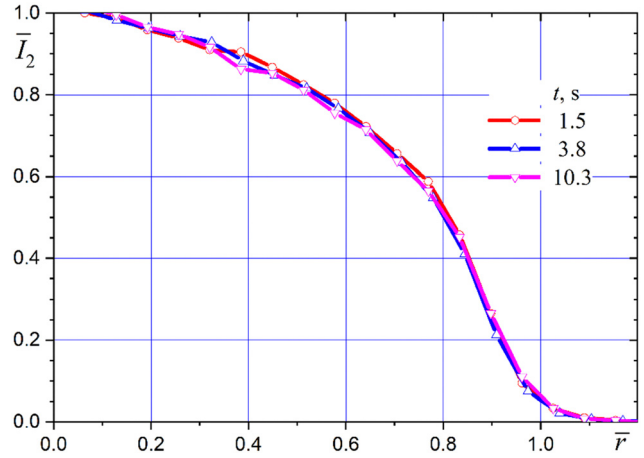

Fig. 9 Universal fluorescence profile of a droplet.

remain significant near caustics, where geometric optics can give physically incorrect results.[37–40]

The transition from the Mie scattering regime to geometrical optics is most clear in the example of a comparatively simple central-symmetric problem when the particle is uniformly illuminated from all sides. In this case, the influence of the fine structure of the absorption field is insignificant and the geometrical optics gives correct results at $x > 100$,[36,39] which are well described by the modified differential approximation taking into account the effect of total internal reflection on the particle surface.[41–43] On the contrary, under the conditions of our experiments, it is better to use the exact Mie solution.

For water droplets illuminated by a parallel beam of light in the visible spectral range, Mie theory gives axisymmetric distributions of absorbed power, which are determined at $x \gg 1$ only by the refractive index of water.[44] The normalized absorption fields for water droplets of radius $a > 8$ μm, which are characterized by the diffraction parameter $x > 100$, are similar. Obviously, this leads to the universal droplet fluorescence profile obtained in the experiments.

If the distribution of the power of absorbed radiation inducing fluorescence over the volume of the droplet is known, the observed fluorescence profile can be calculated using an inverse ray-tracing procedure for a set of parallel rays with different distances from the droplet axis. Most likely, a similar method was used by Frakowiak and Tropea[45] (there is no description of the computational procedure in this brief article).

Each ray, except the axial ray, is refracted on the droplet surface, and the integration of the absorbed radiation power should be performed along the refracted ray. The known equations for reflection and refraction of light at the boundary between transparent, non-scattering media should be used to determine the directions of the rays within the droplet and to account for the reflection of emitted light on the surface of the droplet. It is not necessary to take into account the absorption of this light inside the droplet. Most likely, one can neglect also the multiple reflections of rays in the droplet. Such a computational procedure can become a subject of a separate paper.

The extremely weak absorption of visible light in small water droplets, which simplifies the calculation of fluorescence, also enables us to do without developing a complicated algorithm for determining the field of fluorescein concentration in the droplet volume by the observed fluorescence. It is sufficient to consider the ratio of the measured (possibly non-axisymmetric) image of the fluorescent droplet to the universal brightness profile found above (this is why it was so important to determine this universal profile). The ratio found indicates the position of the zone of increased or decreased fluorescein concentration relative to the vertical symmetry axis of the droplet. Note that we have already used the comparison with the universal fluorescence profile when analyzing the anomalous fluorescence of a large droplet (see Fig. 8). The possibility of quantitative analysis of data on local fluorescence anomalies is expected to be very useful in the experimental study of biochemical processes in the levitating droplets.

5. Conclusions

Fluorescence microscopy with high-resolution and high-speed video imaging was used to study the evolution of fluorescence profiles of microdroplets in levitating droplet clusters. This type of microscopy can be applied for chemical and biochemical investigations of processes in microdroplets without contact with solid surfaces. A universal brightness profile, which does not depend on the droplet temperature and size, was found experimentally. A physical explanation of this universal profile based on the rigorous theory of light scattering was given. A method for determining the parameters of the optical inhomogeneity of a droplet from its fluorescent image was proposed as well. It was demonstrated that this method works for the first observed anomalous luminescence of some large droplets with initially high brightness at the periphery of the droplet. Physical estimates showed that the disappearance of this effect after a few seconds is caused by the diffusion of the fluorescent substance in the water.

Since the 1990s, elaborate techniques of biochemical and biomedical investigation including Fluorescence Recovery After Photobleaching (FRAP), Fluorescence Lifetime Imaging Microscopy (FLIM), and Fluorescence Resonance Energy Transfer (FRET) have been developed. These techniques enable the visualization of complex events in cells. Potentially, a combination of FRAP/FLIM/FRET methods with the levitating droplet cluster may lead to new advances in the study of living systems inside microdroplets. The authors consider the present work as the initial stage of experimental studies of chemical and biochemical processes using new possibilities of aeromicrofluidics and methods of spectral optical diagnostics of semitransparent media.

Conflicts of interest

There are no conflicts to declare.

Acknowledgements

The work was partially supported by the Ministry of Science and Higher Education of the Russian Federation (project no. FEWZ-2023-0002). The authors are grateful to Prof. Rodion Ganopolsky and Dr Paul Nikolaychuk for useful discussions.

References

1 A. A. Fedorets, Droplet cluster, *JETP Lett.*, 2004, **79**(8), 372–374, DOI: **10.1134/1.1772434**.
2 A. A. Fedorets, M. Frenkel, E. Shulzinger, L. A. Dombrovsky, E. Bormashenko and M. Nosonovsky, Self-assembled levitating clusters of water droplets: Pattern-formation and stability, *Sci. Reports*, 2017, **7**, 1888.
3 A. A. Fedorets, E. Bormashenko, L. A. Dombrovsky and M. Nosonovsky, Droplet clusters: Nature-inspired biological reactors and aerosols, *Phil. Trans. R. Soc. A*, 2019, **377**(2150), 20190121, DOI: **10.1098/rsta.2019.0121**.
4 A. A. Fedorets, L. A. Dombrovsky, D. V. Shcherbakov, E. Bormashenko and M. Nosonovsky, Thermal conditions for the formation of self-assembled cluster of droplets over the water surface and diversity of levitating droplet clusters, *Heat Mass Transfer*, 2022, DOI: **10.1007/s00231-022-03261-8**.
5 P. Jiang, R. Chen, X. Zhu, D. Ye, Y. Yang, H. Wang, H. Li, Y. Yang and Q. Liao, Light Droplet Levitation in Relation to Interface Morphology and Liquid Property, *J. Phys. Chem. Lett.*, 2022, **13**, 4762–4767.
6 Z. Wei, Y. Li, R. G. Cooks and X. Yan, Accelerated reaction kinetics in microdroplets: Overview and recent developments, *Ann. Rev. Phys. Chem.*, 2020, **71**, 31–51.
7 Y. Zhang, M. J. Apsokardu, D. E. Kerecman, M. Achtenhagen and M. V. Johnston, Reaction kinetics of organic aerosol studied by droplet assisted ionization: Enhanced reactivity in droplets relative to bulk solution, *J. Am. Soc. Mass Spectr.*, 2021, **32**(1), 46–54, DOI: **10.1021/jasms.0c00057**.
8 K. Li, K. Gong, J. Liu, L. Ohnoutek, J. Ao, Y. Liu, X. Chen, G. Xu, X. Ruan, H. Cheng, J. Han, G. Sui, M. Ji, V. K. Valev and L. Zhang, Significantly accelerated photochemical and photocatalytic reactions in microdroplets, *Cell Rep. Phys. Sci.*, 2022, **3**, 100917, DOI: **10.1016/j.xcrp.2022.100917**.
9 A. A. Fedorets, D. V. Shcherbakov, V. Y. Levashov and L. A. Dombrovsky, Self-stabilization of droplet clusters levitating over heated salt water, *Int. J. Thermal Sci.*, 2022, **182**, 107822.
10 G. Lu and B. Fei, Medical hyperspectral imaging: a review, *J. Biomed. Optics*, 2014, **19**(1), 010901.
11 V. V. Tuchin, *Tissue optics: Light scattering methods and instruments for medical diagnostics*, 3rd edn, SPIE Press, Bellingham, Washington, 2015.
12 W. Zhang, H. Song, X. He, L. Huang, X. Zhang, J. Zheng, W. Shen, X. Hao and X. Liu, Deeply learned broadband encoding stochastic hyperspectral imaging, *Light: Sci. Appl.*, 2021, **10**, 108.
13 *Fluorescence spectroscopy, imaging and probes: New tools in chemical, physical and life sciences*, ed. R. Kraayenhof, A. J. W. G. Visser, H. C. Gerritson, Springer, Berlin, 2002.
14 J. R. Lakowicz, *Principles of fluorescence spectroscopy*, Springer, New York, 3rd edn, 2006.
15 P. P. Mondal and A. Diaspro, *Fundamentals of fluorescence microscopy: Exploring life with light*, Springer, Heidelberg, 2014.
16 C. Maqua, V. Depredurand, G. Castanet, M. Wolff and F. Lemoine, Composition measurements of bicomponent droplets using laser-induced fluorescence of acetone, *Exper. Fluids*, 2007, **43**(6), 979–992.
17 J. Fattaccioli, J. Baudry, J.-D. Émerard, E. Bertrand, C. Goubault, N. Henty and J. Bibette, Size and fluorescence measurements of individual droplets by flow cytometry, *Soft Matter*, 2009, **5**, 2232–2238.
18 F. Lemoine and G. Castanet, Temperature and chemical composition of droplets by optical measurement techniques: a state-of-the-art review, *Exper Fluids*, 2013, **54**(7), 34, DOI: **10.1007/s00348-013-1572-9**.
19 T. Suzuki and J. Kohno, Collisional reaction of liquid droplets: amidation of dansyl chloride observed by fluorescence enhancement, *Chem. Lett.*, 2015, **44**, 1575–1577, DOI: **10.1246/cl.150753**.
20 M. Koegl, C. Weiß and L. Zigan, Fluorescence spectroscopy for studying evaporating droplets using the dye Eosin-Y, *Sensors*, 2020, **20**, 5985, DOI: **10.3390/s20215985**.
21 A. Z. Nelson, B. Kundukad, W. K. Wong, S. A. Khan and P. S. Doyle, Embedded droplet printing in yield-stress fluids, *Proc. Natl. Acad. Sci. U. S. A.*, 2020, **117**(11), 5671–5679, DOI: **10.1073/pnas.1919363117**.
22 S. Shityakov, E. Salvador, G. Pastorin and C. Förster, Blood–brain barrier transport studies, aggregation, and molecular dynamics simulation of multiwalled carbon nanotube functionalized with fluorescein isothiocyanate, *Int. J. Nanomed.*, 2015, **10**, 1703–1713, DOI: **10.2147/ijn.s68429**.
23 S. Shityakov, I. Puskás, K. Pápai, E. Salvador, N. Roewer, C. Förster and J.-A. Broscheit, Sevoflurane-sulfobutylether-beta-cyclodextrin complex: Preparation, characterization, cellular toxicity, molecular modeling and blood–brain barrier transport studies, *Molecules*, 2015, **20**(6), 10264–10279, DOI: **10.3390/molecules200610264**.
24 A. A. Fedorets, L. A. Dombrovsky, E. Bormashenko and M. Nosonovsky, A hierarchical levitating cluster containing transforming small aggregates of water droplets, *Microfluid. Nanofluid.*, 2022, **26**, 52, DOI: **10.1007/s10404-022-02557-9**.
25 L. A. Dombrovsky, A. A. Fedorets and D. N. Medvedev, The use of infrared irradiation to stabilize levitating clusters of water droplets, *Infrared Phys. Technol.*, 2016, **75**, 124–132, DOI: **10.1016/j.infrared.2015.12.020**.
26 L. A. Dombrovsky, A. A. Fedorets, V. Y. Levashov, A. P. Kryukov, E. Bormashenko and M. Nosonovsky, Stable cluster of identical water droplets formed under the infrared irradiation: Experimental study and theoretical modeling, *Int. J. Heat Mass Transfer*, 2020, **161**, 120255, DOI: **10.1016/j.ijheatmasstransfer.2020.120255**.
27 A. P. Demchenko, Photobleaching of organic fluorophores: quantitative characterization, mechanisms, protection, *Methods Appl. Fluoresc.*, 2020, **8**(2), 022001.
28 L. Lindqvist, A flash photolysis study of fluorescein, *Arkiv för Kemi.*, 1960, **16**(8), 79–138.

29 V. Kasche and L. Lindqvist, Reactions between the triplet state of fluorescein and oxygen, *J. Phys. Chem.*, 1964, **68**(4), 817–823, DOI: **10.1021/j100786a019**.
30 R. Y. Tsien and A. Waggoner, *Fluorophores for confocal microscopy, Handbook of biological confocal microscopy*, Springer, Boston, 1995.
31 M. Imamura and M. Koizumi, Irreversible photobleaching of the solution of fluorescent dyes. I. Kinetic studies on the primary process, *Bull. Chem. Soc. Japan*, 1955, **28**(2), 117–124, DOI: **10.1246/bcsj.28.117**.
32 J. J. Shah, M. Gaitan and J. Geist, Generalized temperature measurement equations for rhodamine B dye solution and its application to microfluidics, *Anal. Chem.*, 2009, **81**(19), 8260–8263, DOI: **10.1021/ac901644w**.
33 T. Casalini, M. Salvalaglio, G. Perale, M. Masi and C. Cavallotti, Diffusion and aggregation of sodium fluorescein in aqueous solutions, *J. Phys. Chem. B*, 2011, **115**, 12896–12904, DOI: **10.1021/jp207459k**.
34 H. C. van de Hulst, *Light scattering by small particles*, Dover, New York, 1981.
35 C. F. Bohren and D. R. Huffman, *Absorption and scattering of light by small particles*, Wiley, New York, 1998.
36 W. Hergert and T. Wriedt, *The Mie theory: Basics and applications*, Springer, Berlin, 2012.
37 J. A. Lock and E. A. Hovenac, Internal caustic structure of illuminated liquid droplets, *J. Opt. Soc. Amer. A*, 1991, **8**(10), 1541–1552, DOI: **10.1364/JOSAA.8.001541**.
38 H. M. Lai, P. T. Leung, K. L. Poon and K. Young, Characterization of the internal energy density in Mie scattering, *J. Opt. Soc. Amer. A*, 1991, **8**(10), 1553–1558, DOI: **10.1364/JOSAA.8.001553**.
39 D. Q. Chowdhury, P. W. Barber and S. C. Hill, Energy-density distribution inside nonabsorbing spheres by using Mie theory and geometrical optics, *Appl. Optics*, 1992, **31**(18), 3518–3523, DOI: **10.1364/AO.31.003518**.
40 N. Velesco, T. Kaiser and G. Schweiger, Computation of the internal field of a large spherical particle by use of the geometrical-optics approximation, *Appl. Optics*, 1997, **36**(33), 8724–8728, DOI: **10.1364/AO.36.008724**.
41 L. A. Dombrovsky, Thermal radiation from nonisothermal spherical particles of a semitransparent material, *Int. J. Heat Mass Transfer*, 2000, **43**(9), 1661–1672, DOI: **10.1016/S0017-9310(99)00231-8**.
42 L. A. Dombrovsky, A modified differential approximation for thermal radiation of semitransparent nonisothermal particles: Application to optical diagnostics of plasma spraying, *J. Quant. Spectr. Radiat. Transfer*, 2002, **73**(2–5), 433–441, DOI: **10.1016/S0022-4073(01)00197-2**.
43 L. A. Dombrovsky, Absorption of thermal radiation in large semi-transparent particles at arbitrary illumination of the polydisperse system, *Int. J. Heat Mass Transfer*, 2004, **47**(25), 5511–5522, DOI: **10.1016/j.ijheatmasstransfer.2004.07.001**.
44 L. A. Dombrovsky and D. Baillis, *Thermal radiation in disperse systems: An engineering approach*, Begell House, New York, 2010.
45 B. Frakowiak and C. Tropea, Fluorescence modelling of droplets intersecting a focused laser beam, *Opt. Lett.*, 2010, **35**(9), 1386–1388, DOI: **10.1364/OL.35.001386**.

